PREPARATION AND DEACIDIFICATION PERFORMANCE OF MOLYBDENUM OXIDE-BASED NANOMATERIALS

Jiao DU [1, *], Haishen SUN [2], Lei ZHANG [3], Xinyuan WANG [4], Chunxia CHEN [5], Lihui SUN [6], Junjie QI [7]

The current utilization of petrochemical energy emits a large amount of sulfides and causes acidification pollution, making effective desulfurization crucial. In this study, the effectiveness of nano molybdenum oxide materials in desulfurization is analyzed, and MoOx catalytic materials with oxygen vacancies are prepared by calcining ammonium molybdate precursor. Secondly, this study prepared MoOxNPs/h-BN catalysts using graphene hexagonal boron nitride as a carrier through synthetic techniques. In addition, molybdenum-based ionic liquids are selected as the molybdenum source in the experiment and supported MoO2/h-BN catalysts are prepared using calcination and impregnation methods. Finally, the characterization characteristics, acidic desulfurization effect, and cycling performance of the catalyst are analyzed. In the desulfurization analysis of oxygen deficient MoOx catalytic materials, the higher the temperature, the better the desulfurization effect, and complete acidic desulfurization of dibenzothiophene could be achieved at 130 ℃ for 3.5 hours. In MoOxNPs/h-BN catalyst desulfurization, the best desulfurization effect was achieved when the loading amount was 5wt.%. The MoOxNPs/h-BN catalyst achieved a desulfurization rate of over 97% for all three substrates after 4.5 hours. In MoO2/h-BN acidic desulfurization, higher temperature means better catalyst desulfurization effect. When the temperature condition was 40 ℃ and the time was 1 hour, 100% desulfurization of dibenzothiophene could be achieved. The experiment shows that the prepared nano molybdenum oxide-based micro materials have good acidic desulfurization effect. This research will provide important technical references for the treatment of sulfurized acidic substances and environmental governance.

Keywords: Molybdenum oxide-based micro; Nanomaterials; Deacidification; Desulphurization; Preparation

[1]* Department of Intelligent Manufacturing, Laiwu Vocational and Technical College, Jinan, China, Corresponding author: lwdjhs@163.com
[2] Department of Intelligent Manufacturing, Laiwu Vocational and Technical College, Jinan, China
[3] Department of Intelligent Manufacturing, Laiwu Vocational and Technical College, Jinan, China
[4] Department of Intelligent Manufacturing, Laiwu Vocational and Technical College, Jinan, China
[5] Department of Intelligent Manufacturing, Laiwu Vocational and Technical College, Jinan, China
[6] Department of Intelligent Manufacturing, Laiwu Vocational and Technical College, Jinan, China
[7] Department of Intelligent Manufacturing, Laiwu Vocational and Technical College, Jinan, China

1. Introduction

Petrochemical fuels emit large amounts of sulfur-containing substances during use, leading to environmental damage. Common natural disasters include acid rain, water acidification, and building corrosion [1-2]. Faced with this severe challenge, it is particularly urgent to find and develop efficient sulfide deacidification treatment technologies. At present, various desulfurization technologies have been developed in the industry for the deacidification treatment of sulfides [3]. Among them, desulfurization technologies for common sulfides such as sulfides, thiols, and aliphatic sulfides are relatively mature and have been applied to a certain extent. However, the above technologies still face many limitations, such as the harsh reaction conditions in the treatment of thiophene sulfides, and the pressure exceeding 2Mpa when the operating temperature is above 300 ℃, which increases the process difficulty and operating costs [4]. In recent years, an increasing number of researchers have been continuously exploring new desulfurization pathways [5]. Common methods include adding hydrogen desulfurization to fuel to avoid acidification caused by sulfide emissions, which utilize organic or inorganic acid groups to convert hydrogen sulfide and absorb it through amine substances [6]. However, this type of technology has poor adaptability to aromatic sulfides. In addition, biological desulfurization technology is also used in sulfurization and deacidification treatment, which mainly utilizes biological enzymes in microorganisms to convert sulfides and achieve deacidification effect [7]. Compared to traditional hydrogenation desulfurization technology, this technology has high temperature sensitivity, good adaptability, and is more environmentally friendly. However, the manufacturing cost of catalysts derived from biological desulfurization technology is high, and the treatment effect of some sulfides is average [8]. At present, researchers from all walks of life are focusing on oxidative desulfurization technology, which uses oxidants to oxidize sulfides into corresponding sulfones or sulfoxides, thereby achieving desulfurization and avoiding environmental acidification [9]. At present, Molybdenum Oxide (MoOx) is the focus of research in this field, as it has unique catalytic performance and stability.

In summary, the emissions of petrochemical fuels will result in the removal of a large amount of sulfurized substances, leading to environmental acidification, and effective desulfurization treatment is the key to avoiding acidification. Therefore, in order to solve the problem of sulfide deacidification, this study will use ammonium molybdate as the precursor material, prepare MoOx through high-temperature calcination and other processes, and analyze its desulfurization performance. This study has two innovative points. The first point is to use advanced nanotechnology to prepare Molybdenum Oxide-Based Nanomaterials (MOBNMs) to achieve higher catalytic activity and stability. The second point is to

conduct in-depth research on the desulfurization mechanism of MOBNMs in the desulfurization process, providing theoretical basis for their optimization in practical applications. The research content will provide technical references for the practical application of MOBNMs in the field of environmental protection.

2. Methods and Materials

2.1 Experimental equipment

The X-ray diffractometer (XRD) used in the experimental equipment is the D8 Advance model from Bruker, Germany; The gas chromatography-mass spectrometer (GC-MS) selected is the ISQ 7000 model from Thermo Fisher Scientific in the United States; The UV visible spectrophotometer (UV-Vis) selected is the 752 model from Shanghai Precision Scientific Instrument Co., Ltd. in China; The surface area tester selected is the ASAP 2020 model from Micromeritics in the United States; The transmission electron microscope (TEM) used is Tecnai G2 F20 model from FEI company in the United States; The magnetic stirrer adopts the 85-2 model from Shanghai Sile Instrument Co., Ltd. in China.

2.2 Experimental drugs

The reagents required for the experiment include acetylene black (analytical grade): provided by Merck Chemical Technology (Shanghai) Co., Ltd. Boric acid (A.R.): provided by Shanghai Xianding Biotechnology Co., Ltd. Sodium molybdate dihydrate (A.R.): provided by Honeywell Special Materials (China) Co., Ltd. Ether (99%): provided by Fresenius Kirby (China) Investment Co., Ltd. Anhydrous ethanol (A.R.): provided by Shell Chemical (China) Co., Ltd. Tert Butanol (TBA) (A.R.): provided by Linde Gas (China) Investment Co., Ltd. Dodecane (A.R.): provided by Mitsubishi Chemical Holdings (China) Co., Ltd. Tetradecane (A.R.): provided by AkzoNobel (China) Investment Co., Ltd.

2.3 Experimental methods

2.3.1 Preparation of MoOx catalyst material with oxygen deficiency

Firstly, weigh 3.0g of $(NH4)_6Mo_7O_{24}\cdot 4H_2O$, and then place the sample solution into the prepared oil bath. Control the temperature at 55 ℃ and stir the sample to make it crystallize into a white solid. Next, prepare the tube furnace and place the previous sample in it, maintaining an N_2 atmosphere for heating operation. The speed needs to be controlled at 5 ℃/min and heated to 700 ℃ for 2 hours of continuous heat treatment. Next, the sample is cooled to obtain the final experimental catalytic sample MoOx. Later on, the calcination temperature can also be adjusted to further obtain different series of MoOx-M catalysts, where M is the calcination temperature during the preparation process.

2.3.2 Preparation of h-BN loaded MoOx nanoparticle materials

The synthesis process of Hexagonal Boron Nitride (h-BN): Firstly, boric acid and urea are weighed at 0.6184g and 12.2122g, respectively, and the two substances are mixed and dissolved in 40mL of ultrapure water. Place the sample solution into the prepared oil bath, control the temperature at 55 ℃, and stir the sample to make it crystallize into a white solid. This operation is consistent with the previous heating, with a controlled temperature of 700 ℃, and continuous heat treatment for 2 hours to obtain the final white solid sample h-BN.

In addition, put the prepared urea and boric acid into ultrapure water, followed by $(NH_4)_6Mo_7O_{24}\cdot 4H_2O$. The amounts of boric acid and urea are 0.6124g and 12.2117g, respectively. Simultaneously, MoO_3 with contents of 2wt.%, 5wt.%, and 10wt.% will be placed in $(NH_4)_6Mo_7O_{24}\cdot 4H_2O$. The following operation is consistent with the preparation of MoOx. The final sample solid is obtained by continuously stirring at 55 ℃ and heating under N_2 atmosphere for 2 hours to obtain the final product. This study refers to the product containing n wt.% MoO_3 as n-MoOxNPs/h-BN, where n values are 2, 5, and 10, respectively.

The synthesis process of MoOx: Firstly, dissolve 5.0g of $(NH_4)_6Mo_7O_{24}\cdot 4H_2O$ in 40mL of high-purity water. The sample temperature is controlled at 55 ℃, during which the water needs to be evaporated by stirring to obtain a white sample solid. The sample is placed in a tube furnace for preparation, which also requires maintaining an N_2 atmosphere and heating up to 700 ℃ for a total of 2 hours to obtain the final MoOx product.

2.3.3 Preparation of h-BN loaded MoO2 material

The preparation process of $(C_{16}mim)_2Mo_2O_{11}$ ionic liquid: Firstly, dissolve 1.2098g of $NaMoO_4\cdot 2H_2O$ (equivalent to 5mmol) in 10mL of water. Next, in an ice water bath environment, slowly add a 30% Hydrogen peroxide (H_2O_2) solution with a capacity of 6mL while stirring. Afterwards, dilute Hydrochloric acid (HCI) was used to adjust the pH value of the liquid to 4.2. Next, select 3.4299g of $(C_{16}mim)Cl$ again, with a content of approximately 10mmol, and dissolve it in 15mL of 95% ethanol. Then, the ethanol solution is fused with the previously obtained solution, and a white solid substance can be obtained by stirring and drying. After vacuum filtration, the obtained solid is placed in a vacuum drying oven and dried at a temperature of 50 ℃ for 24 hours. Finally, the obtained light yellow powder is $(C_{16}mim)_2Mo_2O_{11}$ ionic liquid.

The preparation process of h-BN: Firstly, boric acid and urea are dissolved together in 40mL of ultrapure water in a molar ratio of 1:20. Next, stir and recrystallize at a temperature of 55 ℃. Then, transfer the obtained solution to a tube furnace and calcine it at a high temperature of 900 ℃ under a nitrogen atmosphere for 2 hours. In the end, the obtained white powder is the h-BN product.

Synthesis process of 5.2.3X-MoO_2/h-BN catalyst: Firstly, select 5wt.%

$(C_{16}mim)_2Mo_2O_{11}$ and dissolve it in an appropriate amount of dichloromethane solvent. Next, add 0.18g of the previously synthesized h-BN and stir at room temperature for 3 hours to ensure uniform dispersion. Then, place the obtained solution in a 50 ℃ oven for drying treatment until a white powdery product is obtained. Finally, transfer the obtained solid again to a tube furnace and calcine it at different temperatures under a nitrogen atmosphere for a duration of 3 hours. The final product obtained is the X-MoO_2/h-BN catalyst, where X represents different calcination temperatures.

3 Results

3.1 Characterization of MoOx catalyst with oxygen deficiency and analysis of acidic desulfurization

3.1.1 Catalyst characterization and temperature desorption characterization

Fig. 1 shows the oxygen programmed temperature desorption (O_2-TPD) of MoOx material. The results show that temperature rise will cause oxygen vacancies, such as the oxygen absorption peak observed in commercial grade MoOx-700 at 420 ℃, but general MoO_3 does not appear. In the Electron Paramagnetic Resonance (EPR) characterization analysis of the catalyst in Fig. 1 (a), strong EPR signals can be detected, such as the presence of oxygen vacancies at position g=2.003.

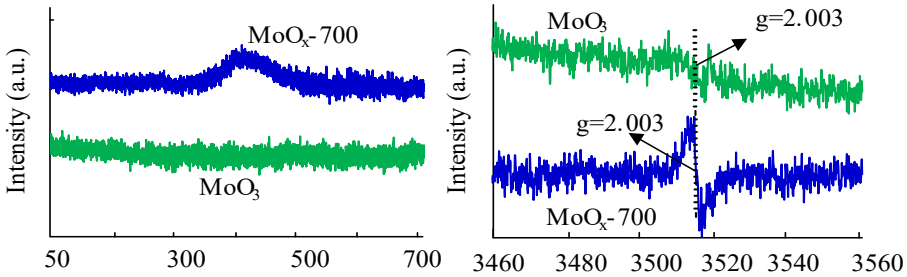

(a) O_2-TPD characterization of MoO_3 and MoOx-700

(b) EPR characterization of MoO_3 and MoOx-700

Fig. 1 Characterization analysis of MoOx material

3.1.2 Desulfurization of commercial grade catalysts at different temperatures

This study selects MoOx-700 material to test the intervention of desulfurization effect at different temperatures, as shown in Fig. 2. The higher the temperature, the higher the desulfurization rate. When the temperature is at 130 ℃ for 3.5 hours, deep desulfurization of Dibenzothiophene (DBT) can be achieved. However, in industry, cost factors need to be fully considered, and generally a

temperature of 120 ℃ is sufficient.

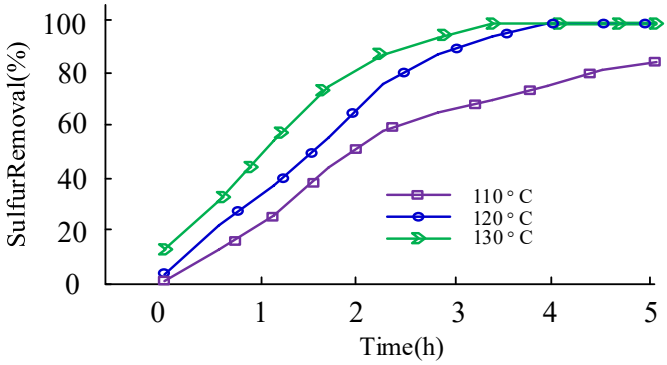

Fig. 2 Comparison of desulfurization effects

3.1.3 Analysis of desulfurization performance under oxygen deficiency

Next, the desulfurization performance under oxygen deficiency will be studied, and the commercial grade MoOx-700 material with better desulfurization performance will still be selected for analysis, and treated in an oxygen rich environment to obtain the treated MoOx. The specific results are shown in Fig. 3. In the UV-Vis of Fig. 3 (a), the desulfurization performance of treated MoOx is significantly reduced compared to untreated MoOx+O_2. UV characterization shows absorption in the MoOx+O_2 region. In the bandgap analysis of Fig. 3 (b), the bandgap width of MoOx+O_2 is 2.82eV, while MoOx is only 1.15eV. This indicates that there is oxygen filling in the bandgap oxygen vacancies, and also suggests that oxygen vacancies have an impact on the desulfurization effect of the catalyst.

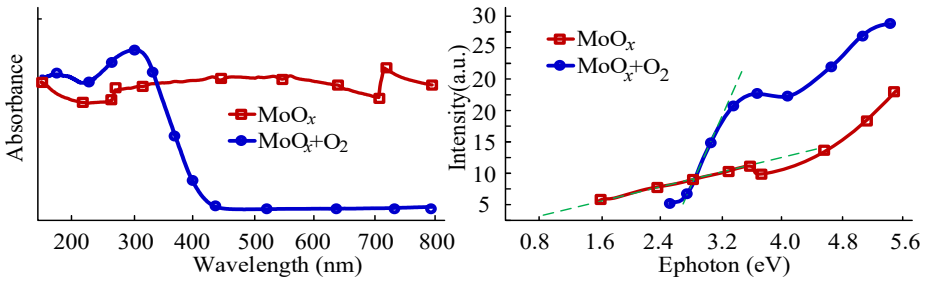

(a) UV spectra of MoOx and MoOx * treated under oxygen enriched conditions

(b) Band gap diagram of MoOx * treated under MoOx and oxygen enriched conditions

Fig. 3 UV-Vis and bandgap diagram of catalyst under oxygen enriched conditions

3.1.4 Comparison of desulfurization of substrates with different sulfur contents

Different sulfur-containing substrates are selected for the experiment,

including 4-Methyldibenzothiophene (4-MDBT), which is commonly found in petroleum fuels. At the same time, 4,6-Methyldibenzothiophene (4,6-DMDBT) and DBT are also added, which are common sulfides, as shown in Fig. 4. The test results show that after 4 hours of treatment, both 4-MDBT and 4,6-DMDBT substrates can achieve desulfurization rates of over 90%, with the highest desulfurization rate being DBT, which can reach 98.25% after 4 hours. The main reasons affecting substrate desulfurization are related to factors such as the electron density of sulfur atoms in the substrate [10].

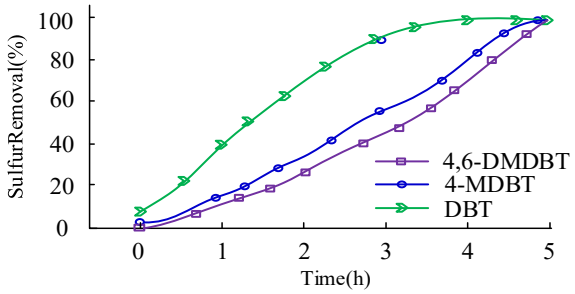

Fig. 4 Comparison of desulfurization properties of different desulfurization substrates

3.1.5 Cyclic testing

The results of testing the cycling ability of MoOx catalyst are shown in Fig. 5. After the first 9 cycles of testing, MoOx still maintains a desulfurization performance of over 98%. Further research found that there is no significant change in the content of Mo particles in the catalyst, but the desulfurization performance decreases with more than 10 cycles, but then increases again. The main reason may be related to the aggregation of catalysts on the substrate surface [11].

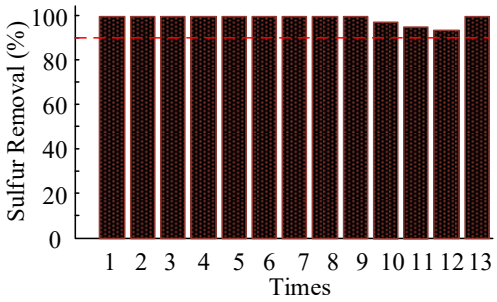

Fig. 5 Catalyst Circulation Ability Test

3.1.6 Reaction mechanism of catalysts

Next, the mechanism of catalyst desulfurization reaction will be studied,

using TBA and Benzoquinone (BQ) as capture agents and conducting quenching experiments, as shown in Fig. 6. After adding TBA, the desulfurization rate remains the same as without any change. After adding BQ, the desulfurization sulfur significantly decreases. This indicates that O_2- is generated. To demonstrate this result, a free radical scavenger test is conducted using pyrroline oxide, as shown in Fig. 6 (b). A weak DMPO-O2- characteristic peak is detected, indicating the presence of free radicals and the oxidation of DBT by O_2-.

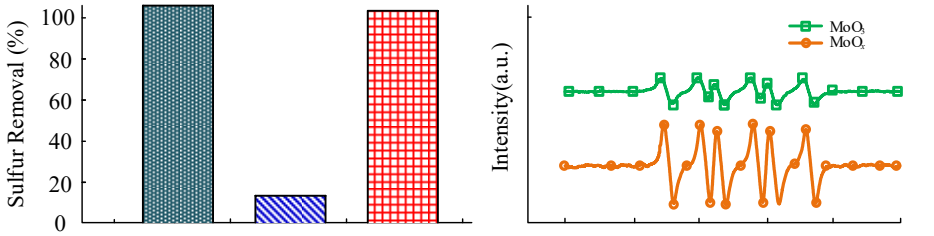

(a) BQ and TBA quenching experiments

(b) Free radical detection in different reaction systems

Fig. 6 Free radical quenching experiment

3.2 Characterization of h-BN loaded MoOx particle material and analysis of acidic desulfurization

3.2.1 Characterization and analysis of catalysts

Fig. 6 shows the characterization of the catalyst under XRD. H-BN exhibits diffraction peaks at 42.1° and 2θ=25.2°, corresponding to the 002 and 100 crystal planes of h-BN. No MoOx peak is found in 5-MoOxNPs/h-BN and 2-MoOxNPs/h-BN. When the load increases by 10wt.%, a MoOx peak appears, indicating successful loading. At 36.8°, a new peak at 10 MoOx/h-BN is observed. Therefore, MoOx catalyst can be well loaded on h-BN without damaging the h-BN structure under MoOx/h-BN.

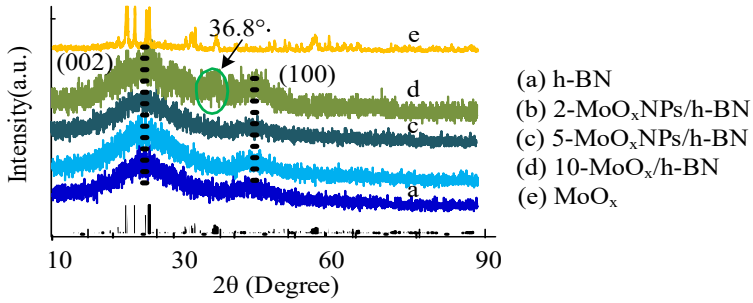

Fig. 7 h-BN, MoO with different loadings, NPs/h-BN (2-10wt.%) XRD characterization results of bulk MoOx

3.2.2 Analysis of desulfurization effects of different loaded catalysts and sulfur-containing substrates

Fig. 8 (a) compares the desulfurization performance of catalysts with different loading amounts. When the load is 5wt.%, the desulfurization rate is significantly improved and can be completely desulfurized in 3 hours. As the load continues to increase, the desulfurization performance of 10-MoOxNPs/h-BN significantly decreases and drops to 77.6%. Therefore, when the load is 5wt.%, it has excellent desulfurization effect, while when the load is 10wt.%, the desulfurization performance gradually decreases. Fig. 8 (b) shows the desulfurization of different substrates by the catalyst. The MoOxNPs/h-BN catalyst achieves a desulfurization rate of over 97% for all three substrates after 4.5 hours. The desulfurization efficiency from high to low is DBT, 4-MDBT, and 4,6-DMDBT, respectively. Further research has shown that the factors affecting substrate desulfurization are mainly related to the density of substrate sulfur atoms and spatial hindrance [12]. For example, 4,6-DMDBT has the highest steric hindrance, resulting in the worst desulfurization performance.

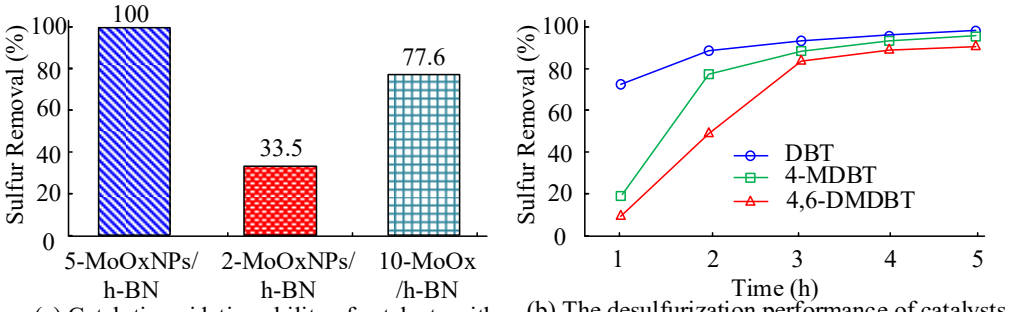

(a) Catalytic oxidation ability of catalysts with different MoOx loadings

(b) The desulfurization performance of catalysts on different substrates

Fig. 8 Analysis of desulfurization effect of different loaded catalysts and sulfur-containing substrates

3.2.3 Cyclic testing

Fig. 9 shows the cyclic performance of the catalyst, which is tested using the 5-MoOxNPs/h-BN catalyst. After 7 cycles, its desulfurization performance is above 97%, but it decreases slightly after 7 cycles. This is mainly related to the aggregation of catalysts on the substrate surface. Therefore, after 8 cycles, the catalyst is cleaned with ether and dried, and the desulfurization performance reaches over 97% in the 9th cycle.

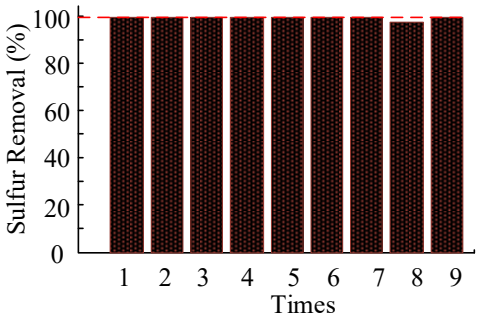

Fig. 9 5-MoOxNPs/h-BN catalyst cyclic performance test

3.2.4 Reaction mechanism of catalysts

Fig. 10 analyzes the reaction mechanism of the catalyst. The experiment uses pyrroline oxide as a spin capture agent and Dimethyl Sulfoxide (DMPO) and BQ as HO· and O_2- capture agents. In the ESR spectrum, the DMPO-O_2- peak can be clearly observed, indicating the presence of active species O_2- in the catalyst reaction. In the quenching experiment, the desulfurization performance significantly decreases with the addition of BQ catalyst, while there is no significant change with the addition of DMSO, indicating that the active species produced in the desulfurization reaction are O_2-.

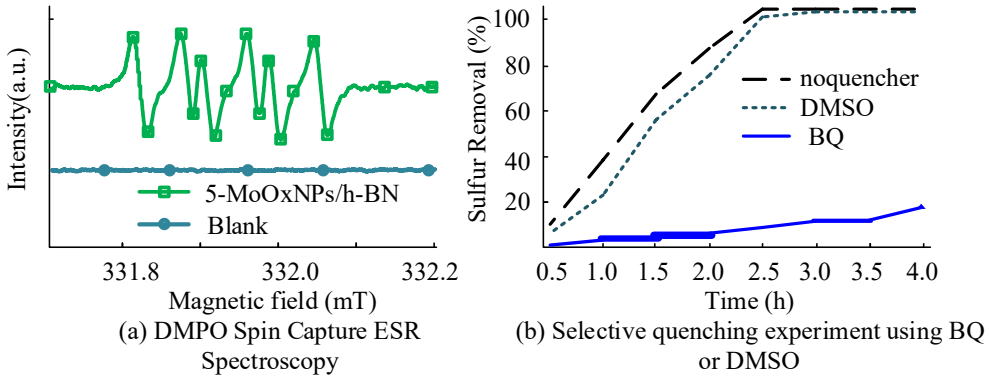

(a) DMPO Spin Capture ESR Spectroscopy

(b) Selective quenching experiment using BQ or DMSO

Fig. 10 Analysis of desulfurization reaction mechanism

3.3 Characterization of h-BN loaded MoOx and analysis of fuel acid desulfurization

3.3.1 Thermogravimetric characterization analysis of precursor

Thermogravimetric characterization analysis is performed on the $(C_{16}mim)_2Mo_2O_{11}$ ion, as shown in Fig. 11. The experiment uses N_2 atmosphere to conduct Thermogravimetry (TG) and Differential Thermogravimetric (DTG)

studies on the precursor. Before the temperature reaches 200 ℃, ions are in a stable state. As the temperature continues to rise, the stable state of particles changes and decomposes, resulting in the first mass loss temperature range of 350 ℃. The process mainly involves the decomposition of long carbon chains. From 370 ℃ to 430 ℃, the second stage of decomposition occurs, which is mainly the decomposition of oxo acid salts, followed by the decomposition of imidazole rings, and finally only molybdenum oxide products remain. The experiment continues to study the decomposition of DTG, which can reflect the rate of mass loss. Each corresponding peak represents the maximum rate of material decomposition, where temperature has a direct impact on the structure of the material after 500 ℃.

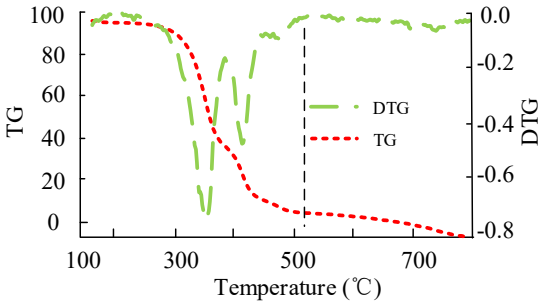

Fig. 11 Thermogravimetric characterization analysis of catalyst

3.3.2 XRD characterization analysis of catalyst

Fig. 12 shows the XRD pattern analysis of the catalyst. At positions 24.9° and 42.8°, h-BN exhibits characteristic peaks belonging to the 002 and 100 crystal planes of h-BN. When the 2θ values are 26.09°, 36.96°, and 53.56°, characteristic peaks are also observed in 700-MoO_2/h-BN, and the characteristics of these peaks are basically consistent with the spectrum of molybdenum oxide under standard conditions. This indicates that the supported catalyst MoO_2/h-BN has been successfully prepared at a calcination temperature of 700 ℃. In the observation of the MoO_2/h-BN spectrum, diffraction peaks of MoO_2/h-BN can be observed, and the h-BN has been successfully loaded with MoO_2. During the calcination preparation process, the temperature rise to 700 ℃ does not cause any damage to the structure. Subsequently, as the temperature increases, the characteristic peak intensity decreases at the curve position of 700-MoO_2/h-BN, and there is a phenomenon of structural damage.

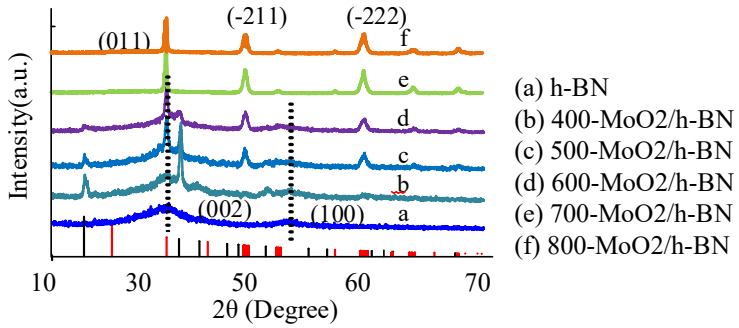

Fig. 12 XRD pattern results of different catalysts

3.3.3 The influence of desulfurization effect under different conditions

The desulfurization effects under different conditions will be compared next, as shown in Fig. 13. This study selects 700-MoO_2/h-BN as the research object. In temperature condition analysis, different temperatures have a significant impact on the desulfurization effect. When the temperature condition increases from 40 ℃ to 60 ℃, the catalyst's sulfur removal efficiency is significantly improved. After 1 hour of desulfurization at a temperature of 40 ℃, DBT can be 100% desulfurized. In addition, different oxidants H_2O_2 are selected to achieve the best desulfurization effect at a temperature of 60 ℃, with a n(O)/n(S) ratio of 4:1. The desulfurization effect on DBT reaches 100% within one hour.

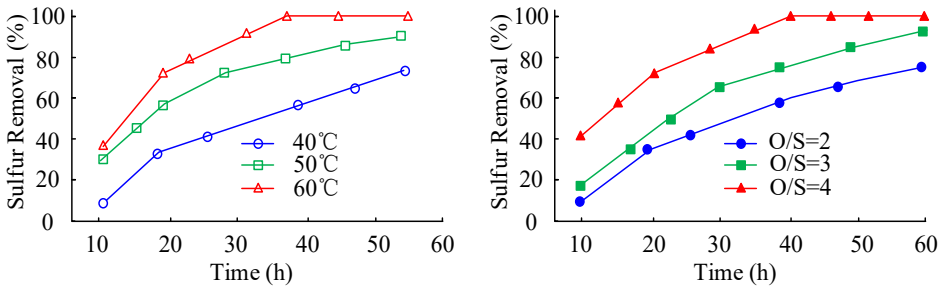

(a) The influence of different temperature desulfurization rates

(b) The influence of different H_2O_2/S molar ratios (n (O)/n (S)) on desulfurization rate

Fig. 13 Comparison of desulfurization effects under different conditions

3.3.4 Oxidation mechanism of catalysts

To accurately determine the active oxides in the desulfurization reaction, BQ and TBA are still selected as capture agents for quenching experiments, as shown in Fig. 14 (a). When TBA is added to the reaction, the desulfurization performance significantly decreases, while BQ does not affect the reaction, resulting in the production of HO during the process. To verify the results, H_2O_2 and MoO_2/h-BN are introduced to continue the experiment. The 1:2:2:1 quadruple

peak of DMPO-HO detected by the spectrum indicates that the final reaction activator is mainly HO free radical.

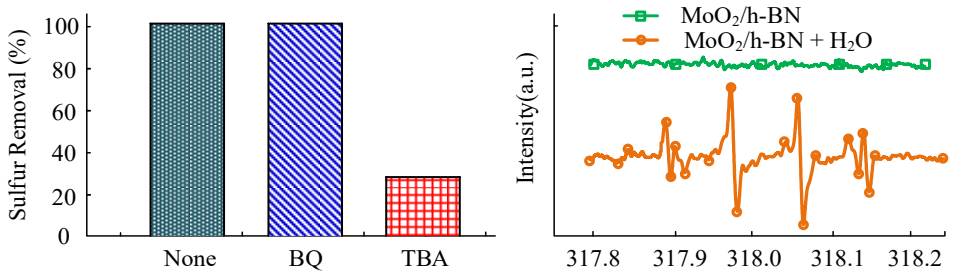

Fig. 14 Selective quenching experiment results

4. Discussion and Conclusion

The inflow of sulfides into the environment is an important factor leading to environmental acidification. The main sulfurized substances in common petroleum fuels include thiols, monocyclic thiophenes, and thioethers [13-14]. In diesel combustion, the main sulfides produced are DBT and its related derivatives [15-16]. These gases react with water vapor in the atmosphere, commonly including H_2SO_4 and other acidic substances, resulting in acid rain and causing significant damage to the environment [17-18]. In addition, sulfur emissions from automobile exhaust and petroleum refining treatment can cause sulfides to penetrate into the soil, leading to increased soil acidification and pollution [19-20]. At present, China's environmental governance is constantly strengthening, and the country has become increasingly strict in controlling the emission of sulfides and acidic pollution from fuel [21-22]. To effectively suppress acidic pollution caused by sulfur pollution, this study prepared an acid desulfurization catalyst using MoOx as a derivative to reduce environmental acidification pollution.

In the study, ammonium molybdate precursor materials were used to prepare MoOx catalyst materials with oxygen vacancies. In the result analysis, MoOx showed excellent performance in desulfurization, and the higher the temperature, the better the catalyst activity. When the temperature was at 130 ℃ for 3.5 hours, deep desulfurization of DBT could be achieved, and the higher the temperature, the better the activity of MoOx catalyst and its desulfurization performance. This was related to the influence of temperature on the structure of the catalyst. In addition, the desulfurization performance of MoOx catalyst significantly decreased after treatment in an oxygen rich environment, indicating that oxygen vacancies have an impact on the desulfurization effect of the catalyst. In the study of the reaction mechanism of MoOx catalyst, it was found that the catalyst mainly achieved the

oxidation treatment of DBT by O_2-, which played an acidic desulfurization effect. In addition, this study prepared MoOxNPs/h-BN catalytic materials by mixing boric acid with ammonium molybdate, and effectively loaded MoOx nanoparticles on the surface of h-BN. Through desulfurization tests under different conditions and cycling performance tests, the prepared MoOxNPs/h-BN catalyst materials have shown good desulfurization performance, with excellent desulfurization performance for substrates DBT, 4-MDBT, and 4,6-DMDBT. The desulfurization mechanism of MoOxNPs/h-BN mainly relied on the oxygen air potential and the adsorption capacity of h-BN, which allowed oxygen and DBT to be adsorbed and form high concentration local DBT. Through oxidation treatment of DBT, the desulfurization effect was effectively achieved. Meanwhile, in this study, $(C16mim)_2Mo_2O_{11}$ was used as the molybdenum source to prepare MoO_2/h-BN with deep desulfurization properties through calcination. By maintaining a temperature of 40 ℃ for 1 hour, DBT could be 100% desulfurized, and its desulfurization oxidation was mainly related to HO free radicals, achieving efficient desulfurization of fuel. Finally, based on literature data analysis, compared with the traditional desulfurization process in Reference [4] that requires high energy consumption conditions of over 300 ℃ and over 2MPa, the ammonium molybdate and h-BN precursors used in the catalyst are easily obtainable in batches, and the calcination and impregnation processes do not require special equipment. They can be adapted to existing industrial production lines and have strong scalability. In terms of cost, the first 9 cycles of MoOx and the first 7 cycles of 5-MoOxNPs/h-BN all maintain high desulfurization rates, reducing replacement costs and lower manufacturing costs compared to the biological desulfurization catalyst in Reference [8]; However, large-scale applications require optimization of continuous reaction equipment to match industrial production capacity.

In summary, MOBNMs have shown great potential for application in terms of deacidification performance. Through preparation and process improvement, it can adapt to the requirements of acid desulfurization treatment under more conditions. The research content will provide technical support for the clean utilization of energy such as oil. Future research also needs to investigate the sulfones produced in the reaction to improve the application effectiveness of the technology.

REFERENCES

[1] Awan A, Baig A, Zubair M, et al. Green synthesis of molybdenum-based nanoparticles and their applications in energy conversion and storage: a review. International Journal of Hydrogen Energy, 2022, 47(72): 31014-31057.

[2] Alam M H, Chowdhury S, Roy A, Wu, X, Ge R. Wafer-scalable single-layer amorphous molybdenum trioxide. ACS nano, 2022, 16(3): 3756-3767.

[3] Avani A V, Anila E I. Recent advances of MoO3 based materials in energy catalysis: Applications in hydrogen evolution and oxygen evolution reactions. International Journal of Hydrogen Energy, 2022, 47(47): 20475-20493.
[4] Liu J, Hui D, Lau D. Two-dimensional nanomaterial-based polymer composites: Fundamentals and applications. Nanotechnology Reviews, 2022, 11(1): 770-792.
[5] Phalswal P, Khanna P K, Rubahn H G, Mishra YK. Nanostructured molybdenum dichalcogenides: a review. Materials Advances, 2022, 3(14): 5672-5697.
[6] Asnag G M, Awwad N S, Ibrahium H A, et al. One-pot pulsed laser ablation route assisted molybdenum trioxide nano-belts doped in PVA/CMC blend for the optical and electrical properties enhancement. Journal of Inorganic and Organometallic Polymers and Materials, 2022, 32(6): 2056-2064.
[7] Zhang Z, Zhao J, Chen Z, Wu, H, Wang S. A molybdenum-based nanoplatform with multienzyme mimicking capacities for oxidative stress-induced acute liver injury treatment. Inorganic Chemistry Frontiers, 2023, 10(4): 1305-1314.
[8] Joseph A, Vijayan A S, Shebeeb C M, Akshay KS. A review on tailoring the corrosion and oxidation properties of MoS 2-based coatings. Journal of Materials Chemistry A, 2023, 11(7): 3172-3209.
[9] Rana A, Pathak S, Lim D K, Kim SK. Recent advancements in plant-and microbe-mediated synthesis of metal and metal oxide nanomaterials and their emerging antimicrobial applications. ACS applied nano materials, 2023, 6(10): 8106-8134.
[10] Sun C, Liu M, Wang L, Li J, Liu S. Revisiting lithium-storage mechanisms of molybdenum disulfide. Chinese Chemical Letters, 2022, 33(4): 1779-1797.
[11] Wondimu T H, Bayeh A W, Kabtamu D M, Xu Q. Recent progress on tungsten oxide-based materials for the hydrogen and oxygen evolution reactions. International Journal of Hydrogen Energy, 2022, 47(47): 20378-20397.
[12] Li M, Zhang P, Guo Z, Cao W, Gao L, Li Y, Tian CF. Molybdenum nanofertilizer boosts biological nitrogen fixation and yield of soybean through delaying nodule senescence and nutrition enhancement. ACS nano, 2023, 17(15): 14761-14774.
[13] Tahir A, Arshad F, Haq T. Roles of metal oxide nanostructure-based substrates in sustainable electrochemical water splitting: Recent development and future perspective. ACS Applied Nano Materials, 2023, 6(3): 1631-1647.
[14] Zhao B, Wu N, Yao S, Yao Y, Lian Ym Li B. Molybdenum carbide/cobalt composite nanorods via a “MOFs plus MOFs” strategy for high-efficiency microwave absorption. ACS Applied Nano Materials, 2022, 5(12): 18697-18707.
[15] Yi S, Guo Y, Li J, Zhang Y, Zhou A, Luo J. Two-dimensional molybdenum carbide (MXene) as an efficient nanoadditive for achieving superlubricity under ultrahigh pressure. Friction, 2023, 11(3): 369-382.
[16] Mishra S R, Ahmaruzzaman M. Tin oxide based nanostructured materials: synthesis and potential applications. Nanoscale, 2022, 14(5): 1566-1605.
[17] Wang Y, Guo X, Li L H. Enhanced piezoelectric properties enabled by engineered low-dimensional nanomaterials. ACS Applied Nano Materials, 2022, 5(9): 12126-12142.
[18] Hameed A, Batool M, Liu Z. Layered double hydroxide-derived nanomaterials for efficient electrocatalytic water splitting: Recent progress and future perspective. ACS Energy Letters, 2022, 7(10): 3311-3328.
[19] Güell F, Galdámez-Martínez A, Martínez-Alanis P R. ZnO-based nanomaterials approach for photocatalytic and sensing applications: recent progress and trends. Materials Advances, 2023, 4(17): 3685-3707.
[20] Jamal F, Rafique A, Moeen S, Haider J. Review of metal sulfide nanostructures and their applications. ACS Applied Nano Materials, 2023, 6(9): 7077-7106.

[21] Aadil M, Kousar T, Hussain M, Somaily HH. Generation of mesoporous npn (ZnO–CuO–CeO2) heterojunction for highly efficient photodegradation of micro-organic pollutants. Ceramics International, 2023, 49(3): 4846-4854.
[22] Zhu J, Ding Y, Ma Z, Deng LM, Wang LQ, Liu SY, Pan H. Recent progress on nanostructured transition metal oxides as anode materials for lithium-ion batteries. Journal of Electronic Materials, 2022, 51(7): 3391-3417.